

A Prototype Scintillating-Fibre Tracker for the Cosmic-ray Muon Tomography of Legacy Nuclear Waste Containers

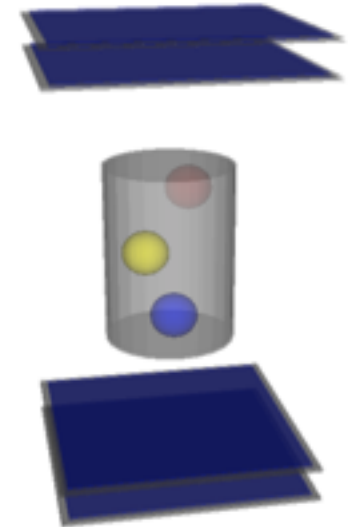
M. Murray, A. Clarkson, D. J. Hamilton, G. D. Hill, M. Hoek, D. G. Ireland, R. Kaiser, T. Keri, S. Lumsden, David F. Mahon, B. McKinnon, S. Nutbeam-Tuffs and G. Yang
Nuclear Physics Group, University of Glasgow, Kelvin Building, University Avenue, Glasgow, G12 8QQ, Scotland, UK

J. R. Johnstone, P. Knight, C. Shearer, C. Staines and C. Zimmerman
UK National Nuclear Laboratory, Central Laboratory, Sellafield, Seascale, Cumbria, CA20 1PG, England, UK

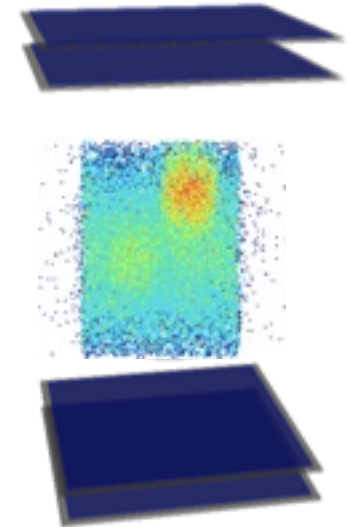
Muon and Neutrino Radiography 2013 (MNR2013)
Detector and Electronics Workshop
Friday 26th July 2013

- UK legacy nuclear waste and the Glasgow MT project
- Glasgow MT detector
 - Design characteristics
 - Construction
 - Performance studies
 - Simulation studies
- Image reconstruction
- Preliminary results and simulation verification
- Summary

- UK legacy nuclear waste and the Glasgow MT project
- Glasgow MT detector
 - Design characteristics
 - Construction
 - Performance studies
 - Simulation studies
- Image reconstruction
- Preliminary results and simulation verification
- Summary



- UK legacy nuclear waste and the Glasgow MT project
- Glasgow MT detector
 - Design characteristics
 - Construction
 - Performance studies
 - Simulation studies
- Image reconstruction
- Preliminary results and simulation verification
- Summary

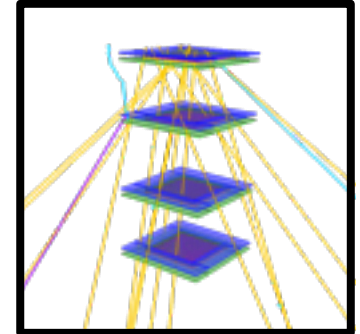
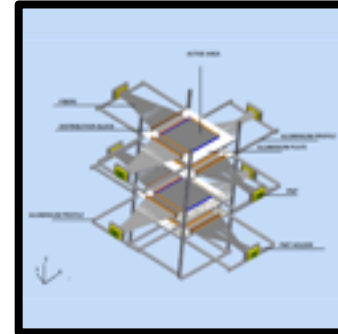


- Currently, there are 8 nuclear power plant facilities operational in the UK
 - 1 Magnox reactor, 6 advanced gas-cooled reactor sites and 1 pressurised-water reactor
 - Government policy is to undertake reactor new-build at several sites within the UK
- A consequence nuclear power is the generation of low-, intermediate- and high-level waste products
 - Legacy silos and waste ponds
 - ILW waste containers (see below)



- The UK's nuclear waste reprocessing is currently performed at Sellafield, Cumbria in the north-west of England
- On Sellafield's site significant volumes of ILW and HLW are stored in highly-engineered structures
- In order to characterise this current (and legacy) waste, techniques to clearly understand waste performance and storage parameters are essential
- Development of characterisation techniques (such as MT) assist in mitigating the risks inherent with long-term storage of these materials

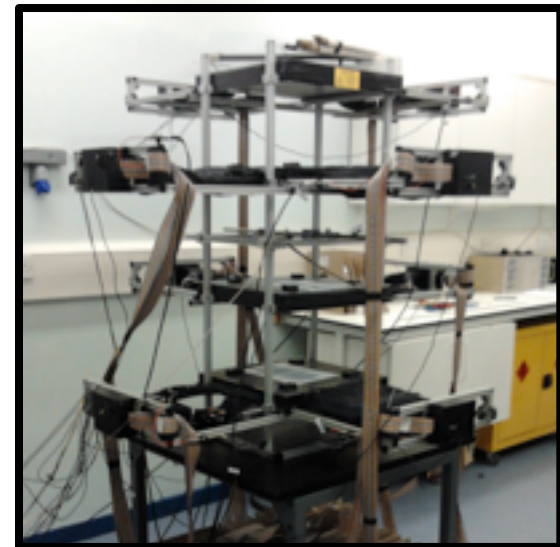
- Industrial collaboration with UK National Nuclear Laboratory (NNL) undertaken on behalf of Sellafield Ltd. (and the UK Nuclear Decommissioning Authority)



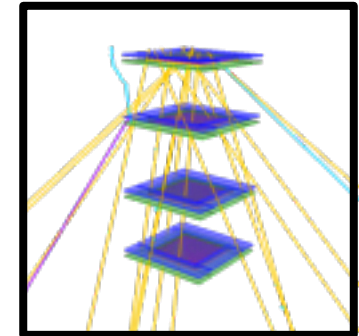
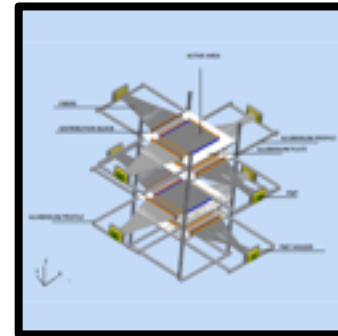
- Began as a feasibility study:

Could a scintillating-fibre MT system be used in the non-destructive assay of legacy nuclear waste containers at Sellafield?

- Small-scale prototype designed and constructed in Glasgow after initial simulation studies confirmed the potential of the technology
- First imaging results on a test setup of objects are presented here



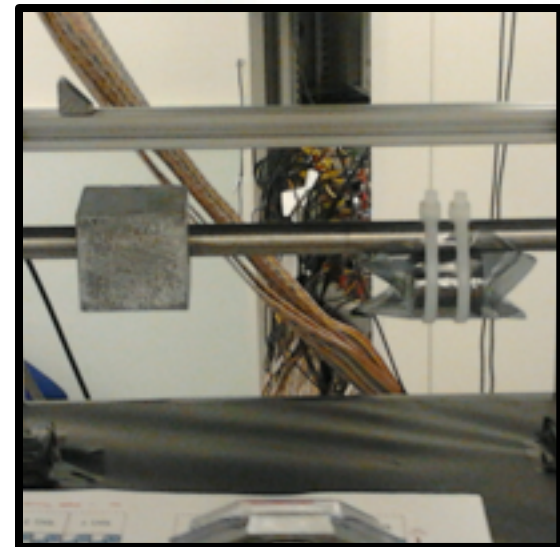
- Industrial collaboration with UK National Nuclear Laboratory (NNL) undertaken on behalf of Sellafield Ltd. (and the UK Nuclear Decommissioning Authority)

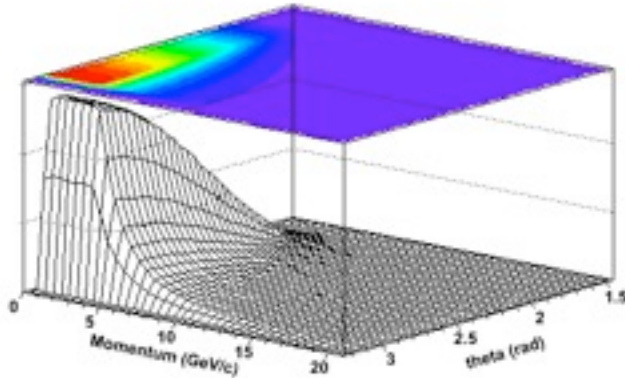


- Began as a feasibility study:

Could a scintillating-fibre MT system be used in the non-destructive assay of legacy nuclear waste containers at Sellafield?

- Small-scale prototype designed and constructed in Glasgow after initial simulation studies confirmed the potential of the technology
- First imaging results on a test setup of objects are presented here



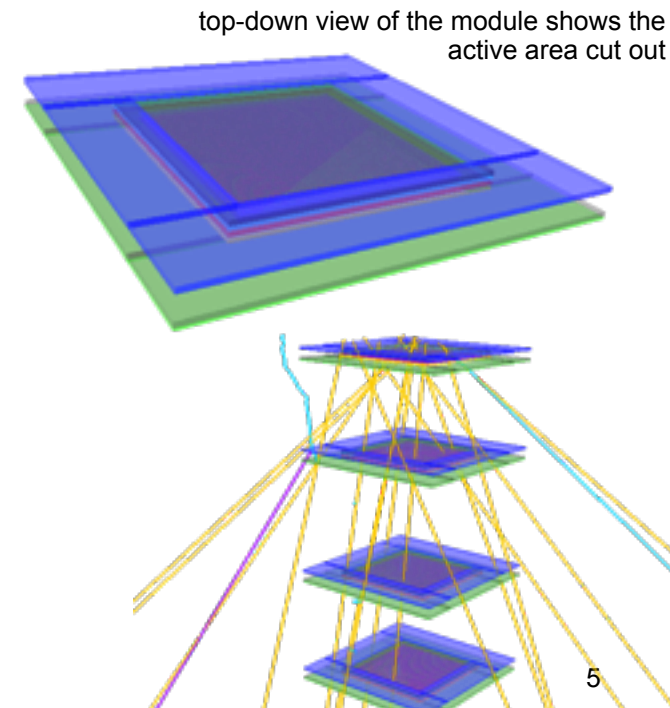


- Cosmic-ray muons are generated by a standalone code based on well established and accurately measured properties:
 - Mean momentum, p_{mean} of 3.35 GeV/c with $p^{-2.7}$ slope at high momenta
 - The angular distribution has a characteristic $\cos^2 \theta$ dependence
 - Muon flux of approximately $1 \text{ cm}^{-2} \text{ min}^{-1}$

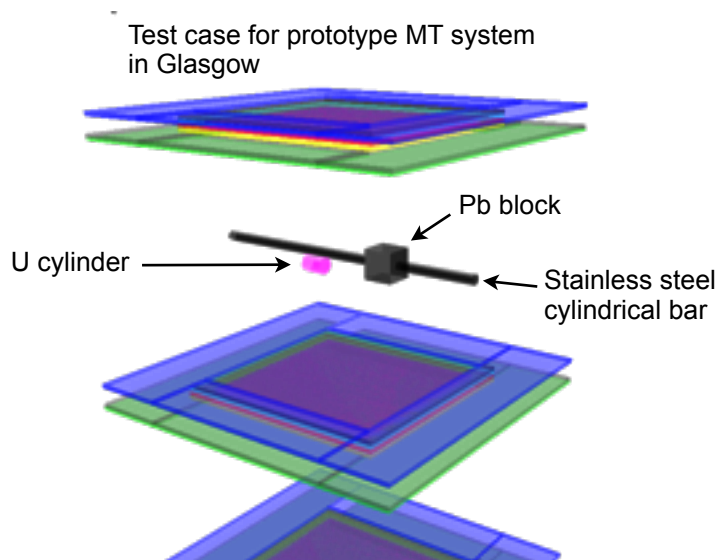
- GEANT4, developed at CERN, is the '*industry standard*' detector simulation framework in particle and nuclear physics
- 'Active' components of the module 'sandwich' structure and materials accurately modelled in GEANT4



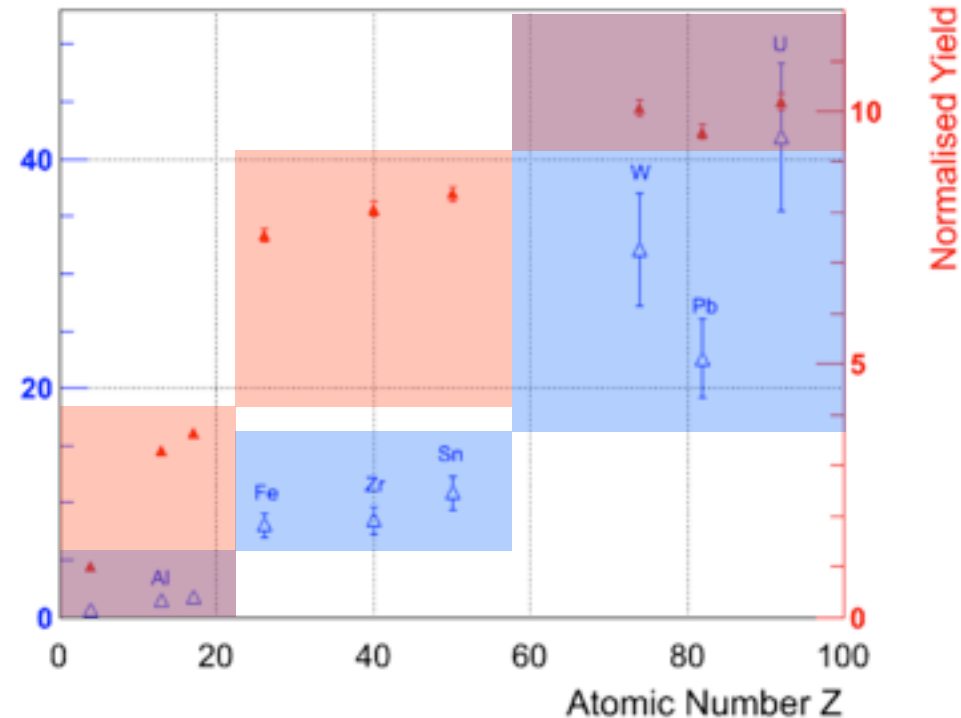
with 'V'-shaped grooves in X-plane (top-side) and Y-plane (under-side)



- Expected material discrimination obtained from GEANT4 simulations studies performed in an air matrix:
 - 10x10x10cm³ blocks of material with 1 day muon exposure
 - Clear separation of low-, medium- and high-Z materials using scattering parameters



λ [mrad²cm⁻¹]

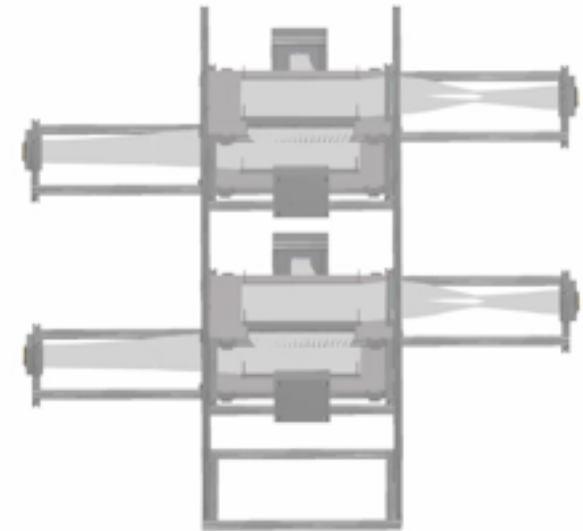
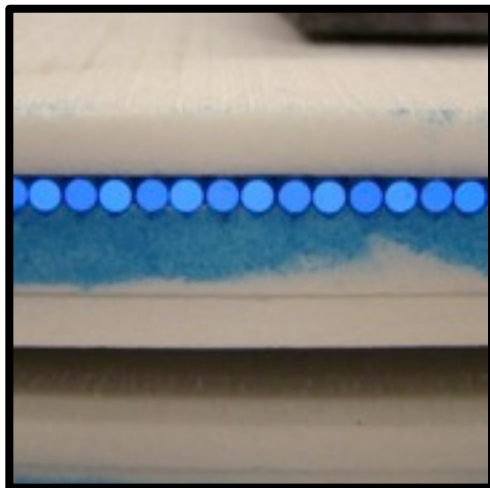


- Experimental test setup in Glasgow simulated (shown opposite without top module)
- Data taking commenced 2012 to verify the initial, promising simulation results

- Prototype detector setup consists of four tracking modules
 - 2 orthogonal layers of 128 scintillating fibres
 - 'Sandwich' structure with flat and machine-grooved Rohacell® (polymethacrylimide) support sheets and Aluminium baseplate



- Layers bonded with optical glue
- Tedlar® and nylon tubing ensure light-tightness

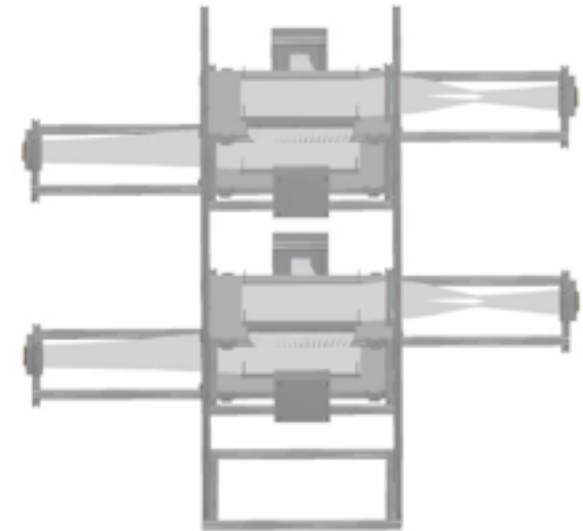
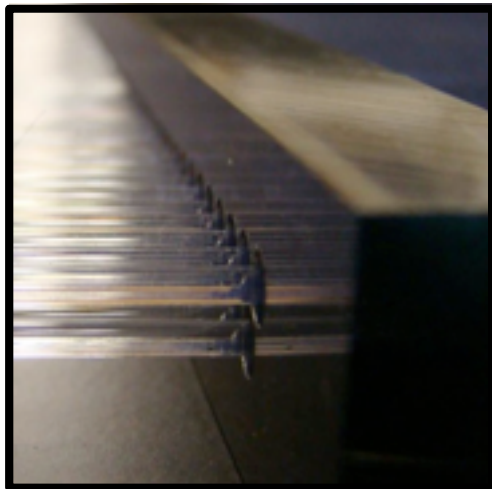


- Fibres held in place by custom-made distribution blocks at edges of Aluminium baseplate and PMT
- All four modules held in place in an Aluminium-profile stand with alignment pins in each module

- Prototype detector setup consists of four tracking modules
 - 2 orthogonal layers of 128 scintillating fibres
 - 'Sandwich' structure with flat and machine-grooved Rohacell® (polymethacrylimide) support sheets and Aluminium baseplate



- Layers bonded with optical glue
- Tedlar® and nylon tubing ensure light-tightness

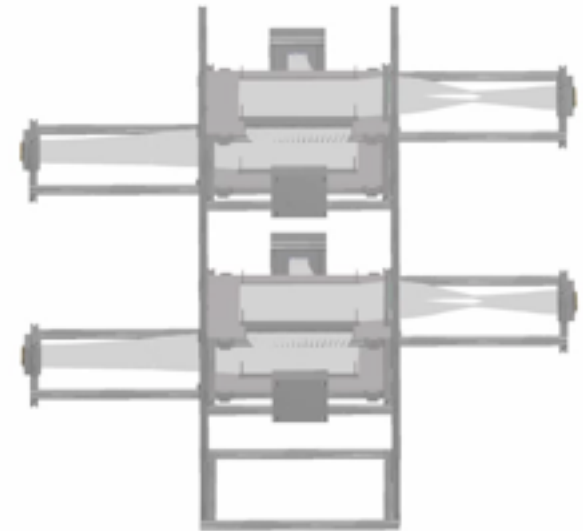
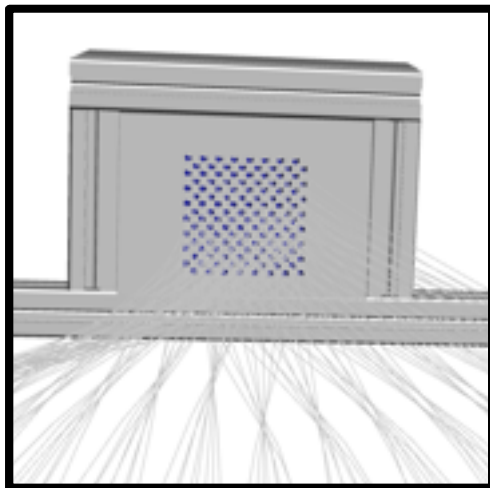


- Fibres held in place by custom-made distribution blocks at edges of Aluminium baseplate and PMT
- All four modules held in place in an Aluminium-profile stand with alignment pins in each module

- Prototype detector setup consists of four tracking modules
 - 2 orthogonal layers of 128 scintillating fibres
 - 'Sandwich' structure with flat and machine-grooved Rohacell® (polymethacrylimide) support sheets and Aluminium baseplate



- Layers bonded with optical glue
- Tedlar® and nylon tubing ensure light-tightness

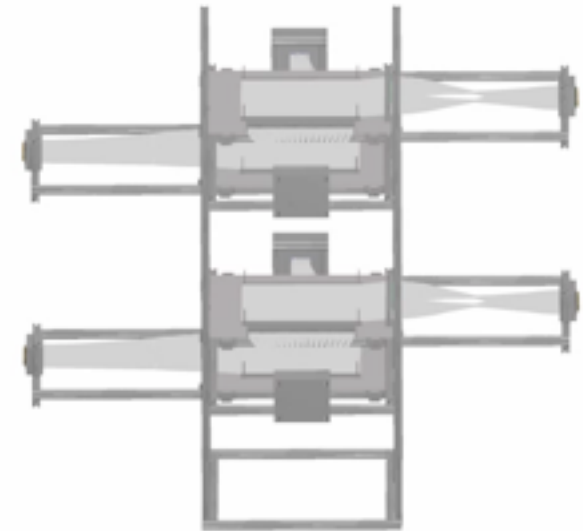


- Fibres held in place by custom-made distribution blocks at edges of Aluminium baseplate and PMT
- All four modules held in place in an Aluminium-profile stand with alignment pins in each module

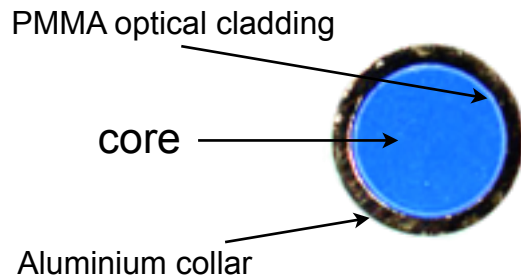
- Prototype detector setup consists of four tracking modules
 - 2 orthogonal layers of 128 scintillating fibres
 - 'Sandwich' structure with flat and machine-grooved Rohacell® (polymethacrylimide) support sheets and Aluminium baseplate




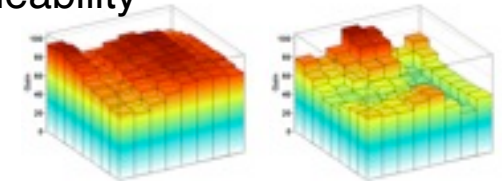
- Layers bonded with optical glue
- Tedlar® and nylon tubing ensure light-tightness




- Fibres held in place by custom-made distribution blocks at edges of Aluminium baseplate and PMT
- All four modules held in place in an Aluminium-profile stand with alignment pins in each module



-  SAINT-GOBAIN scintillating fibres used
 - 2mm pitch with active core of 97% width
 - Polystyrene-based core with PMMA (polymethylmethacrylate) optical cladding (3% width)
- Polished fibre (shown opposite)
- Aluminium collars glued on to ensure uniform contact with PMT
- Chosen for their robustness and scalability

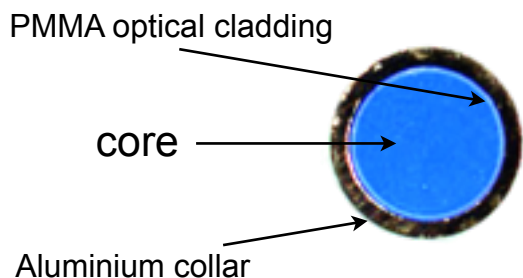



PMT relative-gain maps

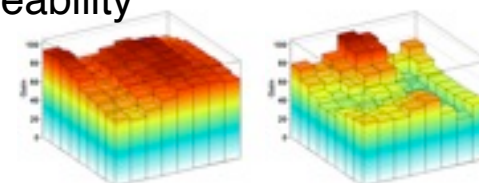
- **HAMAMATSU** H8500 MAPMT (8x8 array segmented anode)
- 2 fibres multiplexed to one pixel via a dedicated coupling scheme to ensure successful fibre identification
- PMTs gain-tested at operational voltages
- Custom-built PCB boards used to read-out to 32-channel  CAEN QDC units




Hamamatsu
H8500 MAPMT (front view)

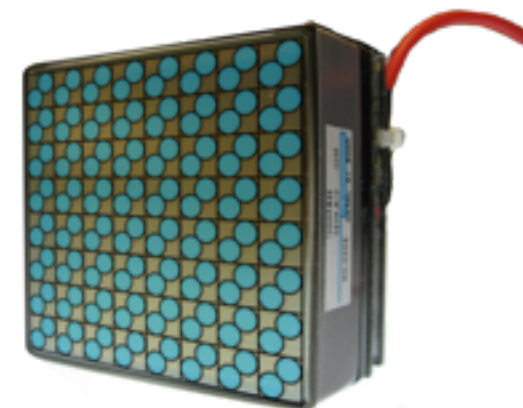


-  SAINT-GOBAIN scintillating fibres used
 - 2mm pitch with active core of 97% width
 - Polystyrene-based core with PMMA (polymethylmethacrylate) optical cladding (3% width)
- Polished fibre (shown opposite)
- Aluminium collars glued on to ensure uniform contact with PMT
- Chosen for their robustness and scalability



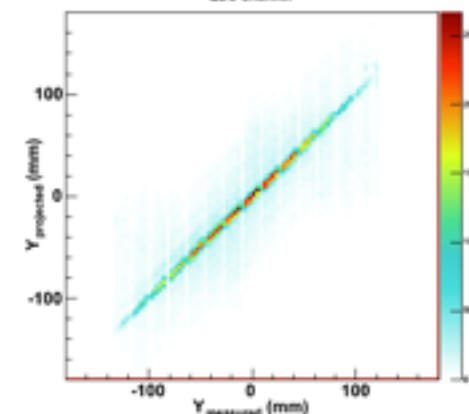
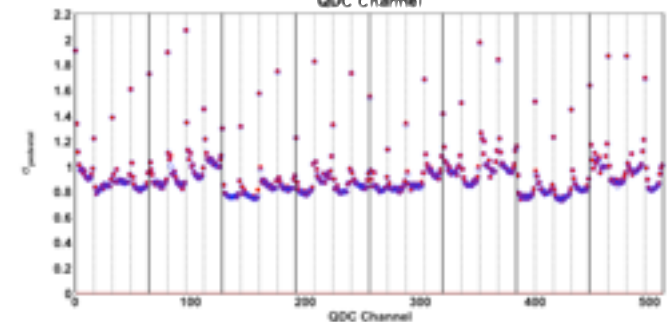
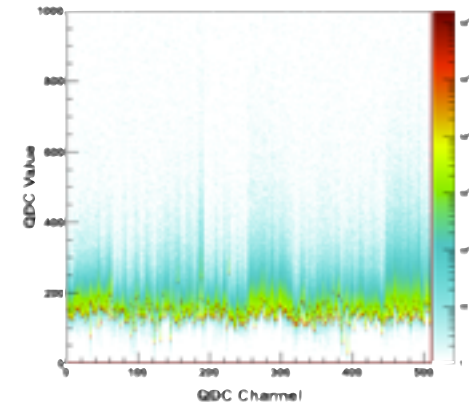
PMT relative-gain maps

- **HAMAMATSU** H8500 MAPMT (8x8 array segmented anode)
- 2 fibres multiplexed to one pixel via a dedicated coupling scheme to ensure successful fibre identification
- PMTs gain-tested at operational voltages
- Custom-built PCB boards used to read-out to 32-channel  CAEN QDC units



Hamamatsu
H8500 MAPMT (front view)

- Multi-fold trigger on Dynode-12 signals from the detector PMTs
- Highest gain-corrected QDC signal above pedestal chosen as 'hit'
- Only events with a hit in each layer are analysed
- Narrow pedestals across the 512 QDC channels
- PMT characterisation and cross-talk investigations completed.
- Relative gain-maps obtained via laser scan
- Multiplicities (~ 1.5 clusters per 1^8 event across all PMTs)
- Detector performance stable over long time periods
- Alignment optimisation undertaken to compensate for minor structural misalignments (less than 5mm)



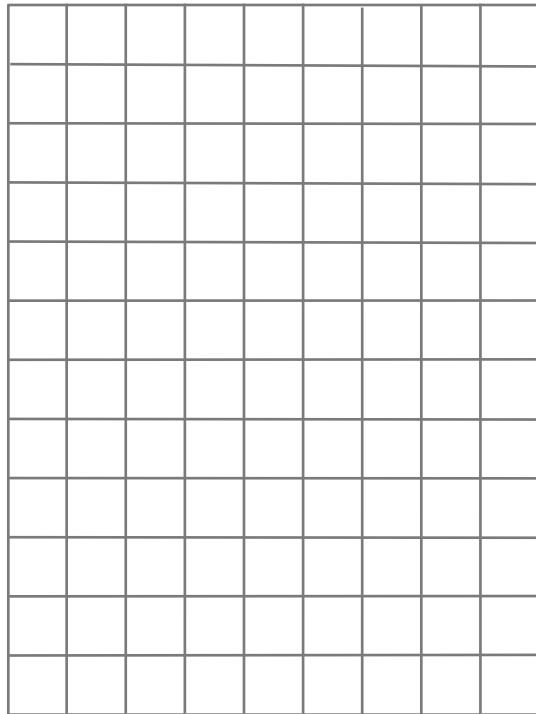
- Imaging volume is split into small volume elements called voxels
- Prior knowledge of the Point of Closest Approach (PoCA) is needed
- This method provides information on every voxel the muon is assumed to have passed through.
- The scattering likelihood of the i th muon in the j th voxel is expressed as:

$$S_{ij}^{(n)} = f(\Delta x, \Delta \theta_x, L_{ij}, T_{ij}, \lambda_j^{(n)})$$

- where Δx and $\Delta \theta_x$ are the spatial and angular deviations of the track (in the x direction) due to scattering, L_{ij} is the pathlength in the voxel, T_{ij} is the 3-D pathlength from the voxel exit point to the exit point from the imaging volume (shown opposite) and $\lambda_j^{(n)}$ is the λ value of the current iteration.
- The λ value of the next iteration is determined as:

$$\lambda_j^{(n+1)} = \frac{1}{M_j} \sum_i S_{ij}^{(n)}$$

- Iteration continues until convergence, i.e. the most likely value has been found.



- Imaging volume is split into small volume elements called voxels
- Prior knowledge of the Point of Closest Approach (PoCA) is needed
- This method provides information on every voxel the muon is assumed to have passed through.
- The scattering likelihood of the i th muon in the j th voxel is expressed as:

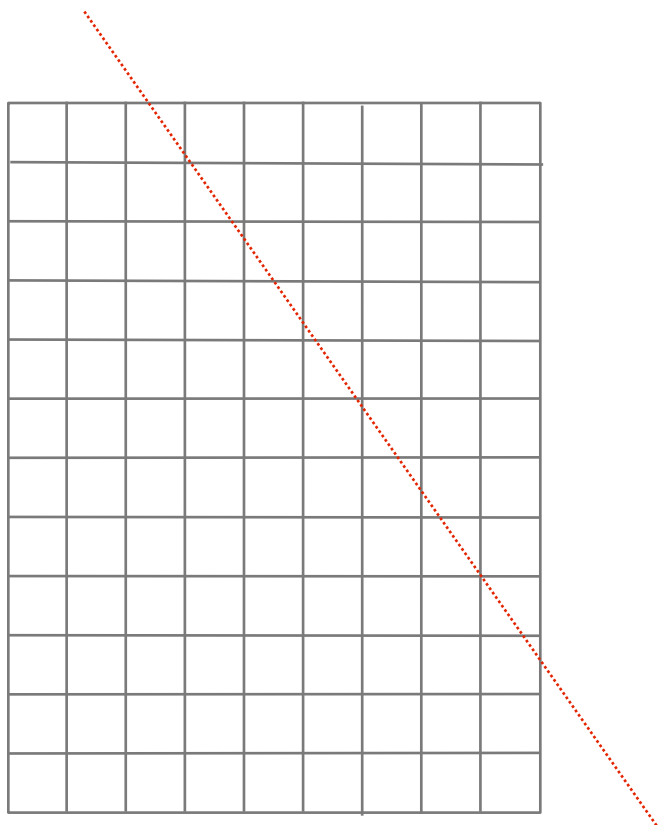
$$S_{ij}^{(n)} = f(\Delta x, \Delta \theta_x, L_{ij}, T_{ij}, \lambda_j^{(n)})$$

- where Δx and $\Delta \theta_x$ are the spatial and angular deviations of the track (in the x direction) due to scattering, L_{ij} is the pathlength in the voxel, T_{ij} is the 3-D pathlength from the voxel exit point to the exit point from the imaging volume (shown opposite) and $\lambda_j^{(n)}$ is the λ value of the current iteration.
- The λ value of the next iteration is determined as:

$$\lambda_j^{(n+1)} = \frac{1}{M_j} \sum_i S_{ij}^{(n)}$$

- Iteration continues until convergence, i.e. the most likely value has been found.

track from top modules



- Imaging volume is split into small volume elements called voxels
- Prior knowledge of the Point of Closest Approach (PoCA) is needed
- This method provides information on every voxel the muon is assumed to have passed through.
- The scattering likelihood of the i th muon in the j th voxel is expressed as:

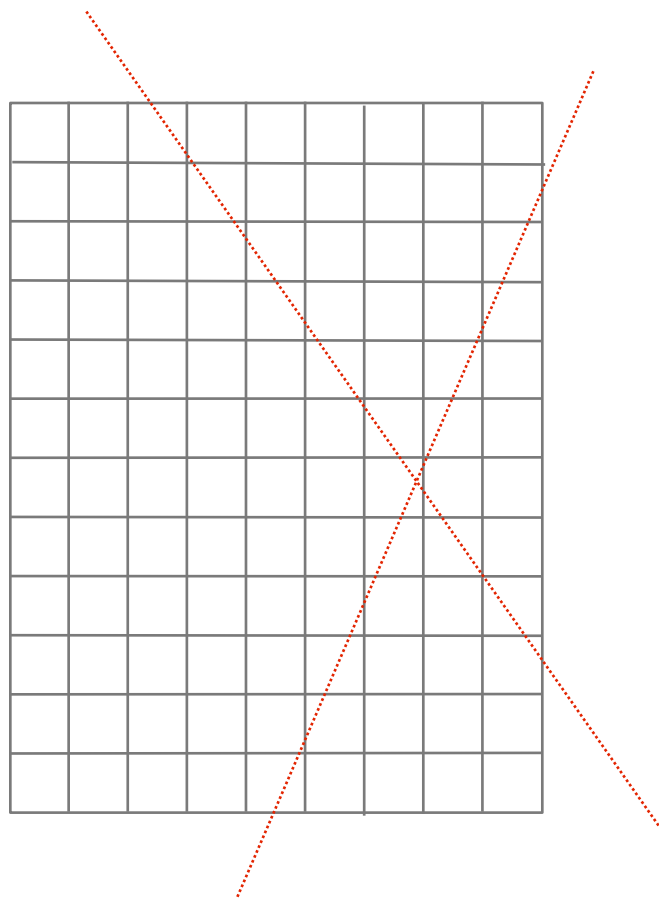
$$S_{ij}^{(n)} = f(\Delta x, \Delta \theta_x, L_{ij}, T_{ij}, \lambda_j^{(n)})$$

- where Δx and $\Delta \theta_x$ are the spatial and angular deviations of the track (in the x direction) due to scattering, L_{ij} is the pathlength in the voxel, T_{ij} is the 3-D pathlength from the voxel exit point to the exit point from the imaging volume (shown opposite) and $\lambda_j^{(n)}$ is the λ value of the current iteration.
- The λ value of the next iteration is determined as:

$$\lambda_j^{(n+1)} = \frac{1}{M_j} \sum_i S_{ij}^{(n)}$$

- Iteration continues until convergence, i.e. the most likely value has been found.

track from top modules



track from bottom modules

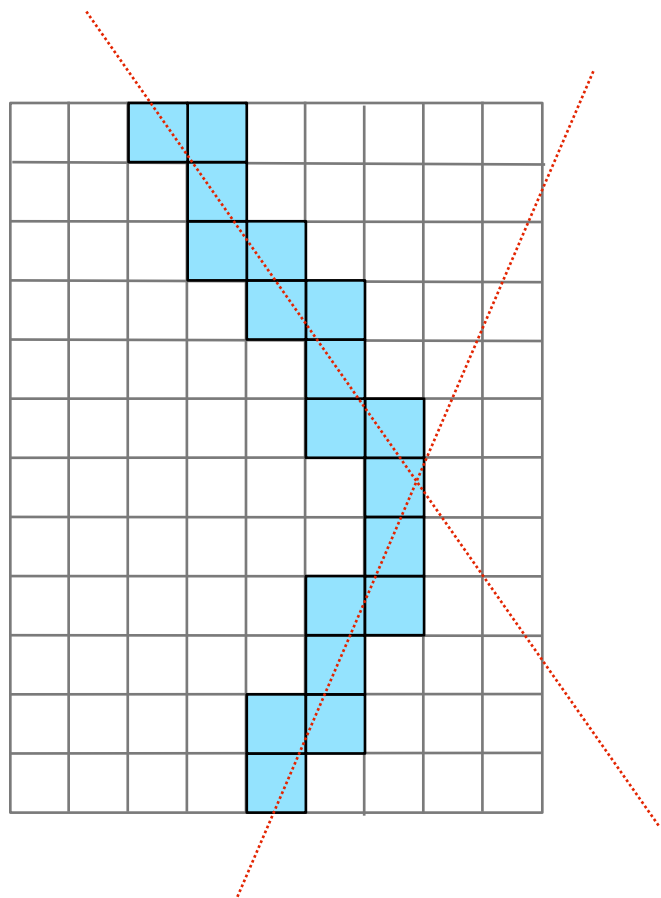
- Imaging volume is split into small volume elements called voxels
- Prior knowledge of the Point of Closest Approach (PoCA) is needed
- This method provides information on every voxel the muon is assumed to have passed through.
- The scattering likelihood of the i th muon in the j th voxel is expressed as:

$$S_{ij}^{(n)} = f(\Delta x, \Delta \theta_x, L_{ij}, T_{ij}, \lambda_j^{(n)})$$

- where Δx and $\Delta \theta_x$ are the spatial and angular deviations of the track (in the x direction) due to scattering, L_{ij} is the pathlength in the voxel, T_{ij} is the 3-D pathlength from the voxel exit point to the exit point from the imaging volume (shown opposite) and $\lambda_j^{(n)}$ is the λ value of the current iteration.
- The λ value of the next iteration is determined as:

$$\lambda_j^{(n+1)} = \frac{1}{M_j} \sum_i S_{ij}^{(n)}$$

- Iteration continues until convergence, i.e. the most likely value has been found.



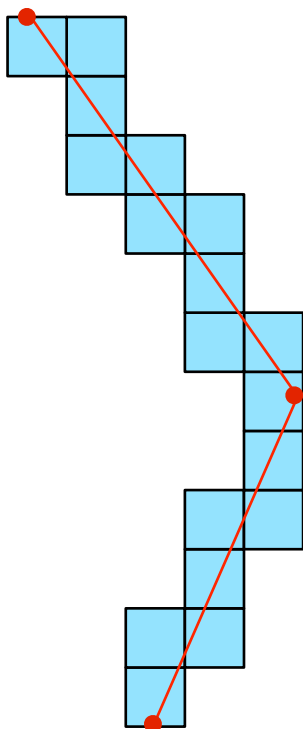
- Imaging volume is split into small volume elements called voxels
- Prior knowledge of the Point of Closest Approach (PoCA) is needed
- This method provides information on every voxel the muon is assumed to have passed through.
- The scattering likelihood of the i th muon in the j th voxel is expressed as:

$$S_{ij}^{(n)} = f(\Delta x, \Delta \theta_x, L_{ij}, T_{ij}, \lambda_j^{(n)})$$

- where Δx and $\Delta \theta_x$ are the spatial and angular deviations of the track (in the x direction) due to scattering, L_{ij} is the pathlength in the voxel, T_{ij} is the 3-D pathlength from the voxel exit point to the exit point from the imaging volume (shown opposite) and $\lambda_j^{(n)}$ is the λ value of the current iteration.
- The λ value of the next iteration is determined as:

$$\lambda_j^{(n+1)} = \frac{1}{M_j} \sum_i S_{ij}^{(n)}$$

- Iteration continues until convergence, i.e. the most likely value has been found.



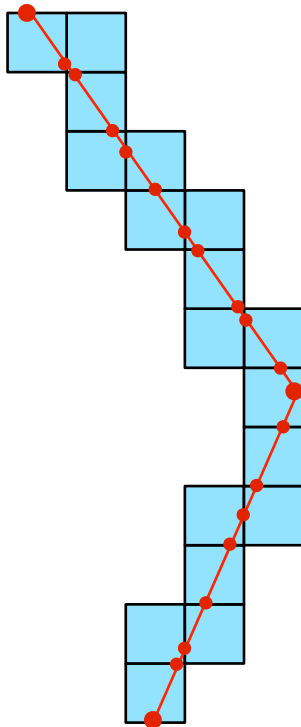
- Imaging volume is split into small volume elements called voxels
- Prior knowledge of the Point of Closest Approach (PoCA) is needed
- This method provides information on every voxel the muon is assumed to have passed through.
- The scattering likelihood of the i th muon in the j th voxel is expressed as:

$$S_{ij}^{(n)} = f(\Delta x, \Delta \theta_x, L_{ij}, T_{ij}, \lambda_j^{(n)})$$

- where Δx and $\Delta \theta_x$ are the spatial and angular deviations of the track (in the x direction) due to scattering, L_{ij} is the pathlength in the voxel, T_{ij} is the 3-D pathlength from the voxel exit point to the exit point from the imaging volume (shown opposite) and $\lambda_j^{(n)}$ is the λ value of the current iteration.
- The λ value of the next iteration is determined as:

$$\lambda_j^{(n+1)} = \frac{1}{M_j} \sum_i S_{ij}^{(n)}$$

- Iteration continues until convergence, i.e. the most likely value has been found.



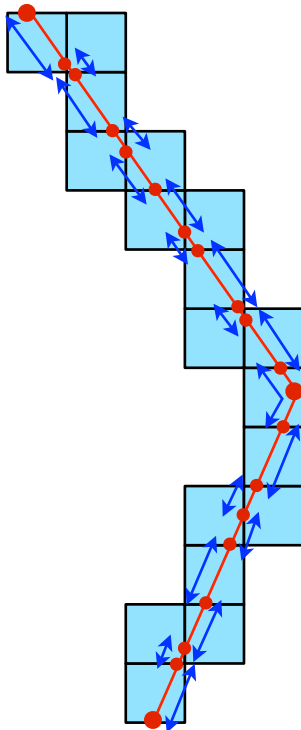
- Imaging volume is split into small volume elements called voxels
- Prior knowledge of the Point of Closest Approach (PoCA) is needed
- This method provides information on every voxel the muon is assumed to have passed through.
- The scattering likelihood of the i th muon in the j th voxel is expressed as:

$$S_{ij}^{(n)} = f(\Delta x, \Delta \theta_x, L_{ij}, T_{ij}, \lambda_j^{(n)})$$

- where Δx and $\Delta \theta_x$ are the spatial and angular deviations of the track (in the x direction) due to scattering, L_{ij} is the pathlength in the voxel, T_{ij} is the 3-D pathlength from the voxel exit point to the exit point from the imaging volume (shown opposite) and $\lambda_j^{(n)}$ is the λ value of the current iteration.
- The λ value of the next iteration is determined as:

$$\lambda_j^{(n+1)} = \frac{1}{M_j} \sum_i S_{ij}^{(n)}$$

- Iteration continues until convergence, i.e. the most likely value has been found.



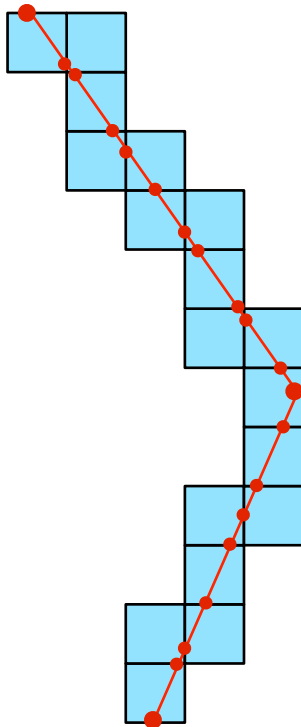
- Imaging volume is split into small volume elements called voxels
- Prior knowledge of the Point of Closest Approach (PoCA) is needed
- This method provides information on every voxel the muon is assumed to have passed through.
- The scattering likelihood of the i th muon in the j th voxel is expressed as:

$$S_{ij}^{(n)} = f(\Delta x, \Delta \theta_x, L_{ij}, T_{ij}, \lambda_j^{(n)})$$

- where Δx and $\Delta \theta_x$ are the spatial and angular deviations of the track (in the x direction) due to scattering, L_{ij} is the pathlength in the voxel, T_{ij} is the 3-D pathlength from the voxel exit point to the exit point from the imaging volume (shown opposite) and $\lambda_j^{(n)}$ is the λ value of the current iteration.
- The λ value of the next iteration is determined as:

$$\lambda_j^{(n+1)} = \frac{1}{M_j} \sum_i S_{ij}^{(n)}$$

- Iteration continues until convergence, i.e. the most likely value has been found.



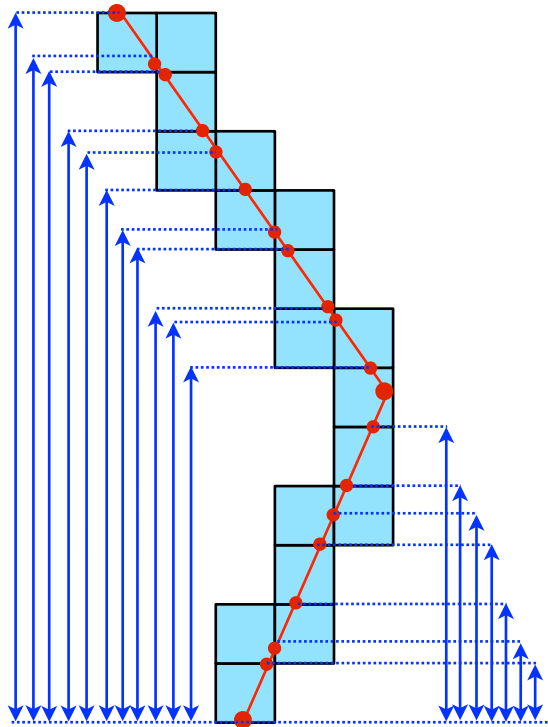
- Imaging volume is split into small volume elements called voxels
- Prior knowledge of the Point of Closest Approach (PoCA) is needed
- This method provides information on every voxel the muon is assumed to have passed through.
- The scattering likelihood of the i th muon in the j th voxel is expressed as:

$$S_{ij}^{(n)} = f(\Delta x, \Delta \theta_x, L_{ij}, T_{ij}, \lambda_j^{(n)})$$

- where Δx and $\Delta \theta_x$ are the spatial and angular deviations of the track (in the x direction) due to scattering, L_{ij} is the pathlength in the voxel, T_{ij} is the 3-D pathlength from the voxel exit point to the exit point from the imaging volume (shown opposite) and $\lambda_j^{(n)}$ is the λ value of the current iteration.
- The λ value of the next iteration is determined as:

$$\lambda_j^{(n+1)} = \frac{1}{M_j} \sum_i S_{ij}^{(n)}$$

- Iteration continues until convergence, i.e. the most likely value has been found.



- Imaging volume is split into small volume elements called voxels
- Prior knowledge of the Point of Closest Approach (PoCA) is needed
- This method provides information on every voxel the muon is assumed to have passed through.
- The scattering likelihood of the i th muon in the j th voxel is expressed as:

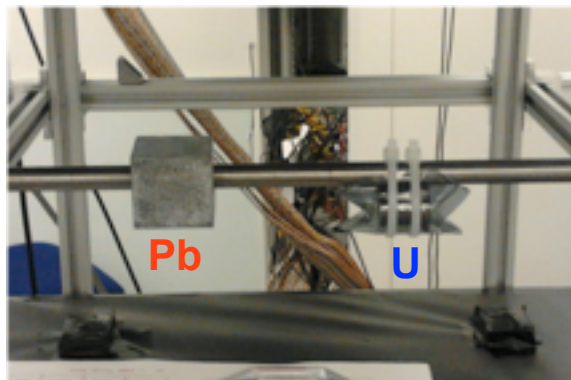
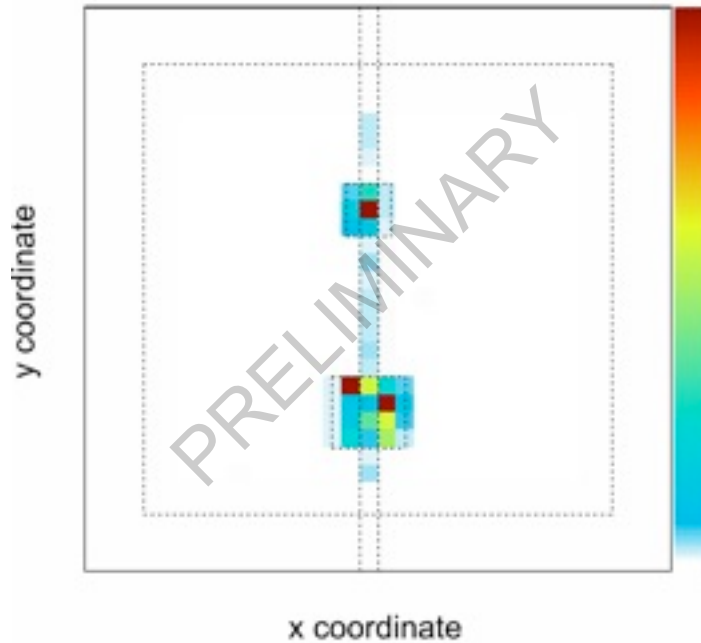
$$S_{ij}^{(n)} = f(\Delta x, \Delta \theta_x, L_{ij}, T_{ij}, \lambda_j^{(n)})$$

- where Δx and $\Delta \theta_x$ are the spatial and angular deviations of the track (in the x direction) due to scattering, L_{ij} is the pathlength in the voxel, T_{ij} is the 3-D pathlength from the voxel exit point to the exit point from the imaging volume (shown opposite) and $\lambda_j^{(n)}$ is the λ value of the current iteration.
- The λ value of the next iteration is determined as:

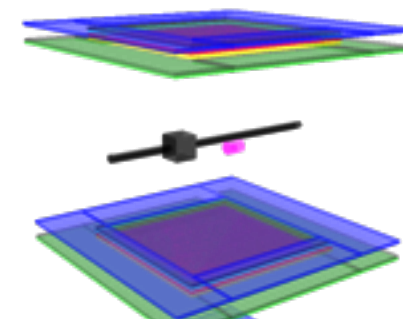
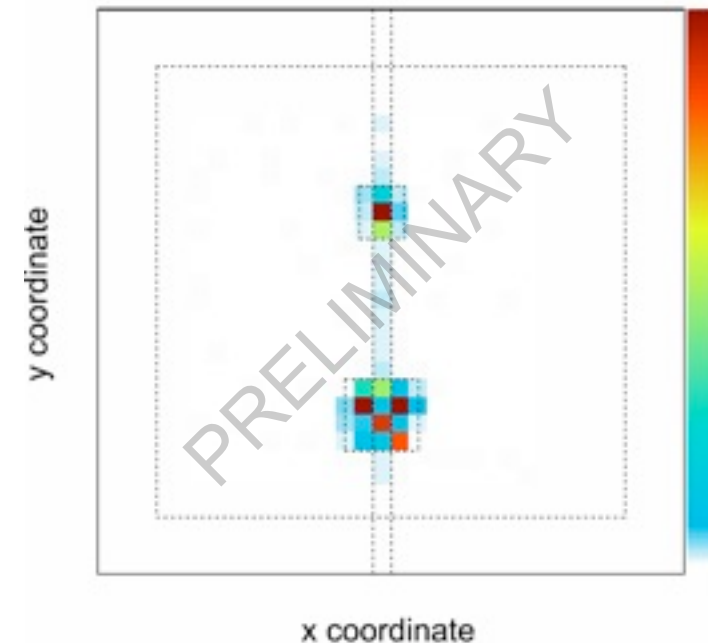
$$\lambda_j^{(n+1)} = \frac{1}{M_j} \sum_i S_{ij}^{(n)}$$

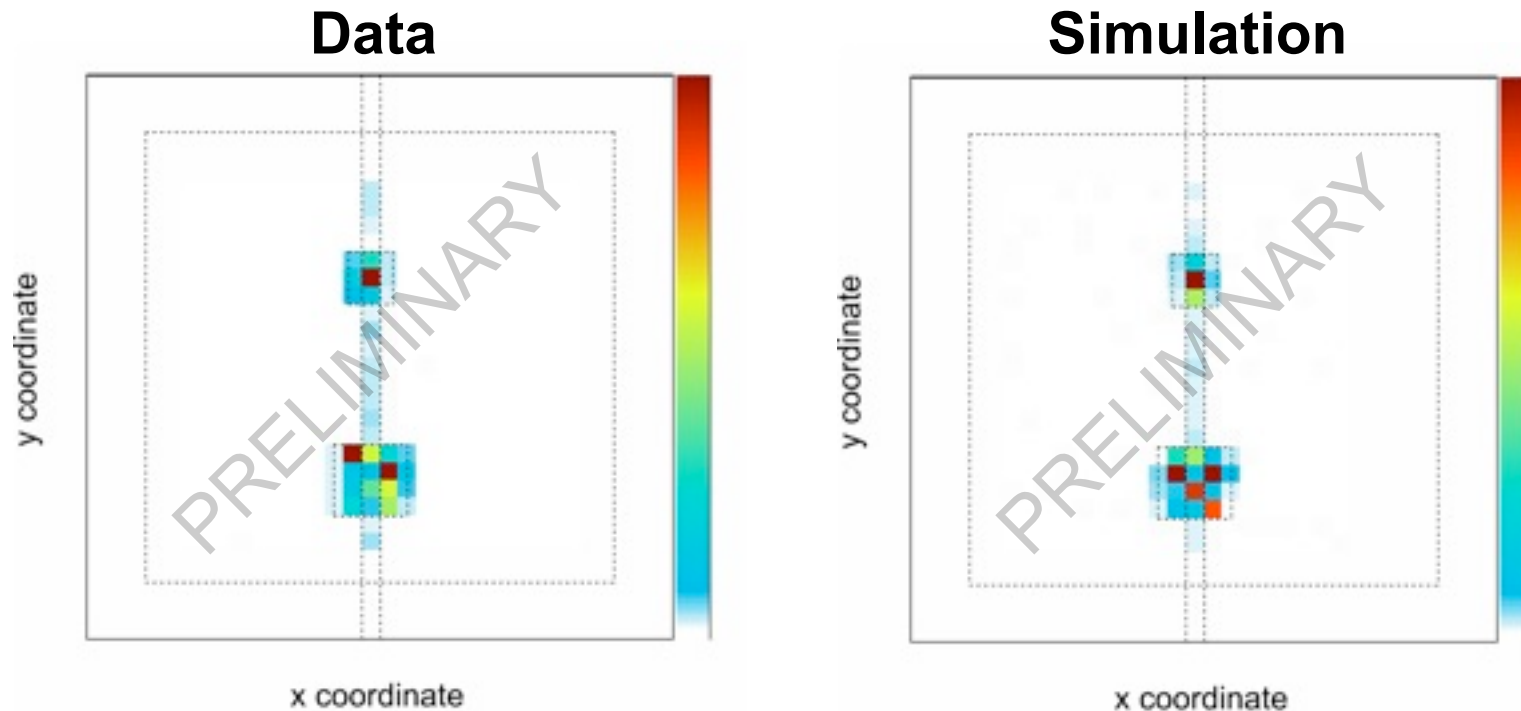
- Iteration continues until convergence, i.e. the most likely value has been found.

Data



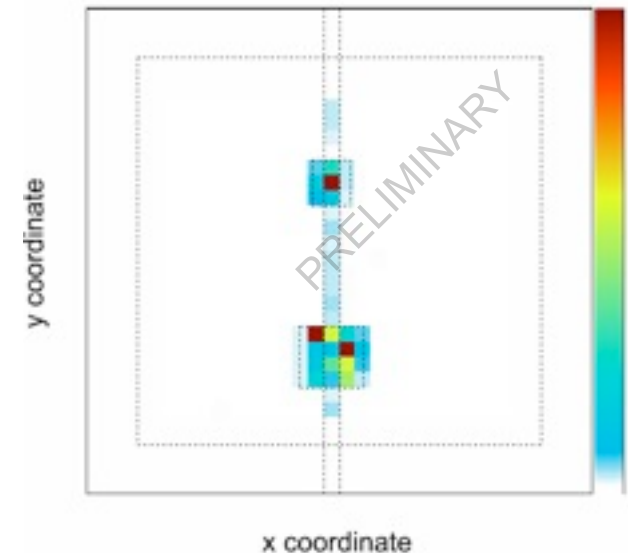
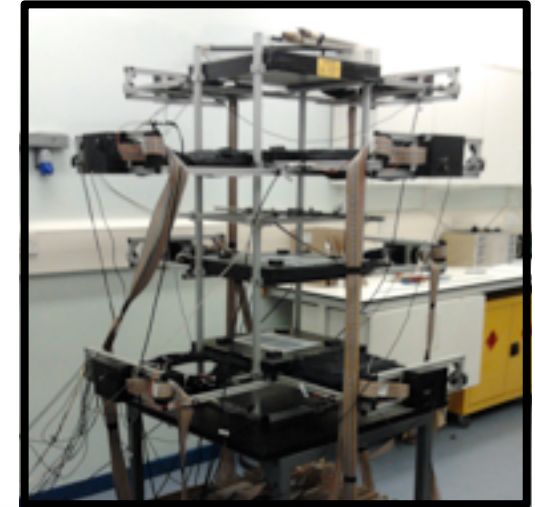
Simulation





- Excellent agreement between the experimental data taken on the prototype detector and the simulated data
- Clear separation observed between the air, steel bar and the two high-Z materials

- Muon tomography is increasingly being used in the non-destructive assay of large and/or shielded objects with applications in fields ranging from archaeology to national security
- In collaboration with the UK National Nuclear Laboratory, the Nuclear Physics group at the University of Glasgow has developed and constructed a prototype MT system using scintillating fibres
- First results from this small-scale prototype in Glasgow verify initial simulation and feasibility studies by discriminating between low-, medium- and high-Z materials
- Work underway on the development of a full-scale detector system with a view to imaging legacy waste containers



I would like to thank the organising committee for giving me the opportunity to present the results and work undertaken by the Nuclear Physics group at the University of Glasgow in collaboration with the UK National Nuclear Laboratory.

In addition, on behalf of the project, I would like to acknowledge the funding contribution from the NDA and Sellafield Ltd. which enabled this research to be undertaken.

